

Kinetics of Nitric Oxide Autoxidation in Aqueous Solution in the Absence and Presence of Various Reductants. The Nature of the Oxidizing Intermediates

Sara Goldstein* and Gidon Czapski

Contribution from the Department of Physical Chemistry, The Hebrew University of Jerusalem, Jerusalem 91904, Israel

Received June 22, 1995[®]

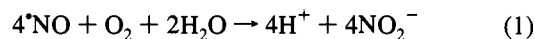
Abstract: The reaction of $\cdot\text{NO}$ with O_2 has been investigated in the absence and presence of various reductants in aqueous solution by the stopped-flow method. The measured yield of nitrite during the autoxidation of $\cdot\text{NO}$ is in agreement with reaction 1: $4\cdot\text{NO} + \text{O}_2 + 2\text{H}_2\text{O} \rightarrow 4\text{NO}_2^- + 4\text{H}^+$. Kinetic studies show that the rate law is $-\text{d}[\text{O}_2]/\text{d}t = k_1[\cdot\text{NO}]^2[\text{O}_2]$ with $k_1 = 2.9 \times 10^6 \text{ M}^{-2} \text{ s}^{-1}$ at 22 °C, which was unaffected by pH and by the presence of either ferrocyanide or ABTS, which are oxidized in this system to ferricyanide and ABTS⁺, respectively. Under limiting concentrations of $\cdot\text{NO}$, the rate law is $-\text{d}[\cdot\text{NO}]/\text{d}t = 4k_1[\cdot\text{NO}]^2[\text{O}_2]$, and it is reduced to $2k_1[\cdot\text{NO}]^2[\text{O}_2]$ in the presence of ferrocyanide or ABTS. The results of the competitive kinetic studies in the presence of ferrocyanide demonstrate that the oxidizing intermediate is $\cdot\text{NO}_2$, whereas in the presence of ABTS both ONOONO, which is the precursor of $\cdot\text{NO}_2$, and $\cdot\text{NO}_2$ are the oxidizing entities. The effect of pH and phosphate buffer concentrations on the oxidation yields and rates suggests the formation of N_2O_3 in these systems, as both OH^- and HPO_4^{2-} enhance the rate of hydrolysis of N_2O_3 . All data were consistent with the formation of ONOONO, $\cdot\text{NO}_2$, and N_2O_3 as oxidizing intermediates during the autoxidation of $\cdot\text{NO}$. The role of each of these intermediates in the oxidation process depends on the relative rates of the reactions of these intermediates with the substrate and those of the different steps of the autoxidation process. A detailed mechanism for the autoxidation of $\cdot\text{NO}$ is given and discussed.

Introduction

Nitric oxide ($\cdot\text{NO}$) is synthesized from L-arginine by many types of cells and is an important mediator in several physiological processes.¹ However, excess production of nitric oxide can be toxic.^{2–7} The cytotoxic and mutagenic effects of $\cdot\text{NO}$ have been attributed largely to the formation of nitrosating and oxidizing agents which are formed via the reaction of $\cdot\text{NO}$ with superoxide and molecular oxygen.^{2–7} The cytotoxic effects of $\cdot\text{NO}$ have also been suggested to result, in part, from S-nitrosation reactions.⁶ It has been demonstrated that $\cdot\text{NO}$ does not react with various thiol-containing compounds to form S-nitroso adducts in the absence of oxygen, whereas the intermediates generated from the $\cdot\text{NO}/\text{O}_2$ reaction nitrosate rapidly a large variety of thiol-containing compounds.^{8,9} The autoxidation of $\cdot\text{NO}$ in aqueous solution is a very complex process, which has not yet been resolved. The nature of the oxidizing and nitrosating intermediates is of great importance

from the biological point of view, and these damaging species have to be identified in order to understand these processes.

The autoxidation of $\cdot\text{NO}$ in aqueous solution produces mainly nitrite with very little nitrate.^{10–15} The overall autoxidation of $\cdot\text{NO}$ has been suggested to occur via reaction 1:



The kinetics of this reaction was studied by several groups by monitoring either the appearance of NO_2^- or the disappearance of $\cdot\text{NO}$.^{10–17} The literature results are in agreement with a rate law which is second order in $\cdot\text{NO}$ and first order in O_2 .^{10–17}

Wink et al.^{9,16} have studied the reaction of $\cdot\text{NO}$ with O_2 in the presence of ferrocyanide, azide, cysteine, and glutathione at pH 7.4. They concluded that the $\cdot\text{NO}/\text{O}_2$ system generates both a strong oxidizing and nitrosating intermediate, NO_x , which is not one of the known nitrogen–oxygen species such as $\cdot\text{NO}_2$, N_2O_3 , NO^+ , or ONOO^- . Pires et al.¹⁴ and Lewis et al.¹⁷ have studied the $\cdot\text{NO}/\text{O}_2$ system in the presence of phenol and morpholine, respectively, and concluded that N_2O_3 is the nitrosating entity.

However, Wink et al.^{9,16} overlooked the effect of phosphate buffer concentration on the product yield, which has been

(10) Pogrebnyaya, V. L.; Usov, A. P.; Baranov, A. V.; Nesterenko, A. I.; Bez'yazychniy, P. I. *J. Appl. Chem. USSR (Engl. Transl.)* **1975**, *48*, 1004.

(11) Awad, H. H.; Stanbury, D. M. *Int. J. Chem. Kinet.* **1993**, *25*, 375.

(12) Ignarro, L. J.; Fukuto, J. M.; Griscavage, J. M.; Rogers, N. E.; Byrns, R. E. *Proc. Natl. Acad. Sci. U.S.A.* **1993**, *90*, 8103.

(13) Lewis, R. S.; Deen, W. M. *Chem. Res. Toxicol.* **1994**, *7*, 568.

(14) Pires, M.; Rossi, M. J.; Ross, D. S. *Int. J. Chem. Kinet.* **1994**, *26*, 1207.

(15) Kahritonov, V. G.; Sundquist, A. R.; Sharma, V. S. *J. Biol. Chem.* **1994**, *269*, 5881.

(16) Wink, D. A.; Darbyshire, J. F.; Nims, R. W.; Saavedra, J. E.; Ford, P. C. *Chem. Res. Toxicol.* **1993**, *6*, 23.

(17) Lewis, R. S.; Tannenbaum, S. R.; Deen, W. M. *J. Am. Chem. Soc.* **1995**, *117*, 3933.

* To whom all correspondence should be addressed.

[®] Abstract published in *Advance ACS Abstracts*, November 15, 1995.

(1) Moncada, S.; Palmer, R. M. J.; Higgs, E. A. *Pharmacol. Rev.* **1991**, *43*, 109–142.

(2) Hibbs, J. B., Jr.; Taintor, R. R.; Vavrin, Z.; Rachlin, E. M. *Biochem. Biophys. Res. Commun.* **1988**, *157*, 87.

(3) Beckman, J. S.; Beckman, T. W.; Chen, J.; Marshall, P. A.; Freeman, B. A. *Proc. Natl. Acad. Sci. U.S.A.* **1990**, *87*, 1620.

(4) Wink, D. A.; Kasprzak, K. S.; Maragos, C. M.; Elespuru, R. K.; Misra, M.; Dunams, T. M.; Cebula, T. A.; Koch, W. H.; Andrews, A. W.; Allen, J. S.; Keefer, L. K. *Science* **1991**, *254*, 1001.

(5) Nowicki, J. P.; Duval, D.; Poignet, H.; Scatton, B. *FEBS Lett.* **1991**, *204*, 339.

(6) Molina y Vedia, L.; McDonald, B.; Reep, B.; Brune, B.; Di Silvio, M.; Billiar, T. R.; Lapetina, E. G. *J. Biol. Chem.* **1992**, *267*, 24929.

(7) Beckman, J. S.; Crow, J. P. *Biochem. Soc. Trans.* **1993**, *21*, 330.

(8) Pryor, W. A.; Church, D. F.; Govindan, C. K.; Crank, G. *J. Org. Chem.* **1982**, *47*, 156.

(9) Wink, D. A.; Nims, R. W.; Darbyshire, J. F.; Christodoulou, D.; Hanbauer, I.; Cox, G. W.; Laval, F.; Laval, J.; Cook, J. A.; Krishna, M. C.; DeGraff, W. G.; Mitchell, J. B. *Chem. Res. Toxicol.* **1994**, *7*, 519.

observed by Lewis et al.¹⁷ Pires et al.¹⁴ neglected the reaction of $\cdot\text{NO}_2$ with $\text{C}_6\text{H}_5\text{O}^-$ to form $\text{C}_6\text{H}_5\text{O}\cdot$ ($k = 8.6 \times 10^6 \text{ M}^{-1} \text{ s}^{-1}$),¹⁸ which may further react with $\cdot\text{NO}$ or $\cdot\text{NO}_2$.^{19,20} Furthermore, some of the studies have the following kinetic errors, which will be discussed in more details later: (i) It has been assumed by mistake that the observed third-order rate constant obtained under limiting concentrations of $\cdot\text{NO}$ is identical to that obtained under limiting concentrations of O_2 .^{9,14,16} (ii) In the formation of N_2O_3 from $\cdot\text{NO}$ and $\cdot\text{NO}_2$, the dissociation of N_2O_3 ²¹ was neglected. This is an unjustified assumption that led to misinterpretation of the results of the competitive kinetics studies.¹⁶ (iii) It was assumed that the rate of formation of the oxidized or nitrosated product is identical to the rate of formation of nitrite in the absence of the various substrates. However, under limiting concentrations of $\cdot\text{NO}$, this rate depends on the nature of the oxidizing or nitrosating intermediate (see below).²²

The goal of this study was to investigate the autoxidation of $\cdot\text{NO}$ in aqueous solutions in the absence and presence of various substrates and to identify the reactive intermediates formed during this process. We will demonstrate that during this process several intermediates are formed, and the one responsible for the oxidation depends on the kind and concentration of the substrate.

Experimental Section

Materials. All chemicals used were of analytical grade and were used as received. Nitric oxide, CP, was purchased from Matheson Gas Products. Solutions were prepared with deionized water that was distilled and purified using a Milli-Q water purification system. Oxygen-saturated solutions (1.2 mM at 22 °C and 690 mmHg, which is the barometric pressure in Jerusalem)²³ were prepared by bubbling gas-tight syringes with oxygen for 30 min. The $\cdot\text{NO}$ gas was purified by passing it through a series of scrubbing bottles containing 50% NaOH and purified water in this order. The solutions in the traps were first deaerated by purging them with helium for an hour. Nitric oxide solutions were prepared in gas-tight syringes by purging first 1 mM phosphate buffer solutions (pH 7.4) with helium to remove O_2 , followed by bubbling for 30 min with $\cdot\text{NO}$. The $\cdot\text{NO}$ -saturated solutions (1.81 mM at 22 °C and 690 mmHg)²³ were stored in syringes and subsequently diluted with helium-saturated solutions to the desired concentrations by the syringe technique. The $\cdot\text{NO}$ -saturated solutions contained contamination of less than 0.1 mM nitrite as determined at 212 nm. The absorption spectra of nitrous acid and nitrite at pH 2 and 7, respectively, were determined. Nitrite has maximum absorption at 212 and 354 nm with $\epsilon = 5100 \pm 100$ and $21 \pm 1 \text{ M}^{-1} \text{ cm}^{-1}$, respectively, in agreement with literature data.^{11,24} Nitrous acid has a maximum absorption at 198 nm with $\epsilon = 1800 \pm 100 \text{ M}^{-1} \text{ cm}^{-1}$ and a structured absorption spectra in the near-UV with a maximum at 372 nm ($\epsilon = 52 \pm 1 \text{ M}^{-1} \text{ cm}^{-1}$). Acetate buffer was used for pH 4.8, phosphate buffer for pH 6–8, HEPES and MOPS buffers for pH 6.8–7.9, and borate buffer for pH 9–10. The acid and alkali pH was adjusted with HClO_4 and NaOH, respectively.

Methods. Stopped-flow kinetic measurements were carried out using The Bio SX-17MV Sequential Stopped-Flow from Applied Photophysics. A Xenon lamp (Osram XBO 150W) produced the analyzing light. Hammamatsu R928 photomultiplier was used for measurements in the near UV- and visible regions. Hammamatsu R166UH photomultiplier (solar blind response) was used for measurements in the far-UV, where the scattered light (stray light) at 216 nm

was about 0.5%, whereas using the R928 photomultiplier, it exceeds 35% and with appropriate filters 5%. If nitrite is present due to contamination of $\cdot\text{NO}$ solutions, the percentage of scattered light increases further as nitrite has a high absorption at 216 nm. The formation of NO_2^- and HNO_2 was followed at 216 nm using $\epsilon = 4900 \pm 100$ and $1150 \pm 50 \text{ M}^{-1} \text{ cm}^{-1}$, respectively. The experiments with relatively high $[\cdot\text{NO}]_0$ (which contains contamination of nitrite) were carried out at low $[\text{O}_2]_0$ ($\Delta\text{OD}_{216} < 0.1$), otherwise the measured yield of nitrite is considerably lower than the real yield due to scattered light.²⁵ The formation of ferricyanide and ABTS⁺ (ABTS = 2,2'-azinobis(3-ethylbenzthiazoline-6-sulfonic acid) was followed at 420 nm ($\epsilon = 1000 \text{ M}^{-1} \text{ cm}^{-1}$) and 660 nm ($\epsilon = 12,000 \text{ M}^{-1} \text{ cm}^{-1}$),²⁶ respectively. The optical path length was 1 cm. All measurements were carried out at 22 °C. Each value given is an average of at least five measurements.

Pulse radiolysis experiments were carried out with the Varian 7715 linear accelerator with 5 MeV electrons pulses of 0.2–0.5 μs and 200 mA current with doses ranging from 2.8 to 8.8 Gy, respectively. A 200-W Xenon lamp produced the analyzing light. The thiocyanate dosimeter was used taking $G(\text{SCN}^-) = 6.1$ and $\epsilon_{475} = 7850 \text{ M}^{-1} \text{ cm}^{-1}$. Irradiations were carried out in a 2- or 4-cm spectrocell using three light passes. We used this technique to determine the rate constant of the reaction of $\cdot\text{NO}_2$ with ferrocyanide and ABTS at pH 7.4 (5 mM phosphate buffer). The reaction of $\cdot\text{NO}_2$ with ferrocyanide and ABTS was studied in deaerated solutions containing 0.5 M nitrate and 0.05 M nitrite. Under these conditions, e_{aq}^- and $\cdot\text{OH}$ are converted into $\cdot\text{NO}_2$, whereas H^\cdot is converted into $\cdot\text{NO}$.²⁸ The reaction of $\cdot\text{NO}_2$ with ferrocyanide was also studied in deaerated solutions containing 0.01 M nitrate and 0.1–1 M *tert*-butyl alcohol. The detailed systems were described elsewhere.²⁹

Results and Discussion

The Mechanism of the Autoxidation of $\cdot\text{NO}$. The mechanism of the autoxidation of $\cdot\text{NO}$ under limiting concentrations of either $\cdot\text{NO}$ or O_2 was studied by following the formation of nitrite or nitrous acid at 216 nm at pH 1.7–11.7. In the presence of excess of O_2 over $\cdot\text{NO}$, the formation of nitrite obeyed a second-order rate law, independent of $[\cdot\text{NO}]_0$, pH, and phosphate concentration (Table 1). The observed rate constant depends linearly on $[\text{O}_2]_0$, (Figure 1A), yielding a slope of $(1.15 \pm 0.06) \times 10^7 \text{ M}^{-2} \text{ s}^{-1}$. The yield of nitrite was found to be linearly

(25) If at a given wavelength (λ) there are $x\%$ scattered light (stray light) coming from wavelengths where the solution does not absorb, $\epsilon_{\text{measured}}(\lambda)$ is smaller than the real value, and for small absorption, $\epsilon_{\text{measured}}(\lambda) = \epsilon_{\text{real}}(\lambda)/(1 + x/100)$. This effect is common in the UV region ($\lambda < 220 \text{ nm}$), where the light intensity is low and a relative high percentage of scattered light is present. This effect is amplified when the solution has an appreciable absorption in the UV, which leads to the inner filter effect, which diminishes further the light intensity. This effect often causes artifacts of absorption peaks in the UV region. The kinetics are also affected by the presence of scattered light. For small absorption, the observed first-order rate constant is not affected, but the second-order rate constant is smaller than the real value because $k(2\text{nd}) = k_{\text{obs}}\epsilon_{\text{measured}}(\lambda)$. In cases where larger absorptions are measured, the first-order rate constant is also affected, but to a much lesser extent than the second-order rate constant. The observed first-order rate constant of formation of absorption increases whereas that of the decay of absorption decreases.

(26) The spectrum of ABTS⁺ obtained via the oxidation of ABTS by $\cdot\text{NO}_2$ in deaerated solutions containing 0.5 M nitrate and 0.05 M nitrite at pH 7.4 (5 mM phosphate buffer) depended on $[\text{ABTS}]_0$. In the presence of $[\text{ABTS}]_0 < 0.2 \text{ mM}$, the absorption maxima of ABTS⁺ are at 416 nm ($\epsilon = 36000 \pm 3600 \text{ M}^{-1} \text{ cm}^{-1}$), which is identical to that determined in the peroxidase– H_2O_2 system in the presence of 0.05 mM ABTS,²⁷ 654 nm ($\epsilon = 12500 \pm 1300 \text{ M}^{-1} \text{ cm}^{-1}$), and 734 nm ($\epsilon = 15000 \pm 1500 \text{ M}^{-1} \text{ cm}^{-1}$), assuming $G(\text{ABTS}^+) = 6.1$. The absorption maxima were shifted toward 420, 660, and 740 nm at $[\text{ABTS}]_0 > 0.5 \text{ mM}$. The extinction coefficient at 420 nm decreased by 40% whereas those at 660 and 740 nm decreased by 10% with the increase in $[\text{ABTS}]_0$ from 0.2 to 5 mM. Therefore, the kinetic measurements were carried out at 660 nm using $\epsilon = 12000 \text{ M}^{-1} \text{ cm}^{-1}$. We have also determined $\epsilon_{600} = 9600 \pm 900 \text{ M}^{-1} \text{ cm}^{-1}$, which is about 45% higher than that used by Wink et al.¹⁶

(27) Childs, R. E.; Bardsley, W. G. *Biochem. J.* **1975**, *145*, 93.

(28) Buxton, G. V.; Greenstock, C. L.; Helman, W. P.; Ross, A. B. *J. Chem. Phys. Ref. Data* **1988**, *17*, 513.

(29) Forni, L. G.; Mora-Arellano, V. O.; Packer, J. E.; Willson, R. L. *J. Chem. Soc., Perkin Trans. 2* **1986**, 1.

(18) Huie, R. E.; Neta, P. *J. Phys. Chem.* **1986**, *90*, 1193.

(19) Janzen, E. G.; Wilcox, A. L.; Manoharan, V. *J. Org. Chem.* **1993**, *58*, 3597–3599.

(20) Huie, R. E. *Toxicology* **1994**, *89*, 193.

(21) Von Gratzel, M.; Taniguchi, S.; Henglein, A. *Ber. Bunsenges. Phys. Chem.* **1970**, *74*, 488.

(22) Goldstein, S.; Czapski, G. *Free Radical Biol. Med.* **1995**, *19*, 785.

(23) *Lange's Handbook of chemistry*, 13th ed.; Dean, J. A., Ed.; McGraw-Hill: New York, 1985; pp 10–5.

(24) Seddon, W. A.; Fletcher, J. W.; Sopchysyn, F. C. *Can. J. Chem.* **1973**, *51*, 1123.

Table 1. The Yield and the Observed Rate Constant of the Formation of Nitrite during the Autoxidation of *NO

[*NO] ₀ , M	[O ₂] ₀ , M	pH	[phosphate], mM	ΔOD ₂₁₆ ^a	Δ[nitrite]/[*NO] ₀ ^b	k _{obs} , s ⁻¹
6.56 × 10 ⁻⁵	1.09 × 10 ⁻³	7.4	1.5	0.33	1.03	2.78
6.56 × 10 ⁻⁵	1.09 × 10 ⁻³	7.4	7.5	0.33	1.03	2.69
6.56 × 10 ⁻⁵	1.09 × 10 ⁻³	7.4	37.5	0.33	1.03	2.51
6.46 × 10 ⁻⁵	1.09 × 10 ⁻³	7.4	75	0.32	0.99	2.53
4.10 × 10 ⁻⁵	1.09 × 10 ⁻³	7.4	1.5	0.20	1.00	2.57
3.28 × 10 ⁻⁵	1.09 × 10 ⁻³	7.4	7.5	0.16	0.99	2.55
2.46 × 10 ⁻⁵	7.26 × 10 ⁻⁴	7.4	1.5	0.10	0.83	1.82
2.46 × 10 ⁻⁵	3.63 × 10 ⁻⁴	7.4	1.5	0.095	0.79	0.86
1.64 × 10 ⁻⁵	1.09 × 10 ⁻³	7.4	7.5	0.083	1.03	2.72
1.64 × 10 ⁻⁵	5.45 × 10 ⁻⁴	7.4	3.75	0.078	0.97	1.28
1.64 × 10 ⁻⁵	2.73 × 10 ⁻⁴	7.4	1.75	0.086	1.06	0.68
2.05 × 10 ⁻⁵	1.09 × 10 ⁻³	11.7	-	0.075	0.75	2.50
4.10 × 10 ⁻⁵	1.09 × 10 ⁻³	1.7	-	0.038	0.81	11.4
1.64 × 10 ⁻³	2.7 × 10 ⁻⁶	7.4	1.6	0.053	4.00	7.20
1.64 × 10 ⁻³	5.4 × 10 ⁻⁶	7.4	1.6	0.107	4.04	7.34
8.20 × 10 ⁻⁴	5.4 × 10 ⁻⁶	7.4	1.6	0.097	3.67	1.91
4.10 × 10 ⁻⁴	5.4 × 10 ⁻⁶	7.4	1.6	0.098	3.70	0.43
4.10 × 10 ⁻⁴	1.08 × 10 ⁻⁵	7.4	1.6	0.22	4.15	0.41
2.05 × 10 ⁻⁴	1.08 × 10 ⁻⁵	7.4	1.6	0.19	3.59	0.095
2.05 × 10 ⁻⁴	5.4 × 10 ⁻⁶	7.4	1.6	0.096	3.63	0.088

^a The change in the absorbance at the end of the reaction. ^b Δ[NO₂⁻] and Δ[HNO₂] were calculated using ε₂₁₆ = 4900 and 1150 M⁻¹ cm⁻¹, respectively.

dependent on [*NO]₀, and Δ[NO₂⁻]/[*NO]₀ = 0.97 ± 0.06 (Table 1). In the presence of excess concentrations of *NO over O₂, the formation of nitrite obeyed a first-order rate law, and Δ[NO₂⁻]/[O₂]₀ = 3.83 ± 0.21 (Table 1). The measured yields of nitrite are in agreement with that expected according to reaction 1. The observed rate constant was found to be linearly dependent on [NO]² (Figure 2A), yielding a slope of (2.9 ± 0.1) × 10⁶ M⁻² s⁻¹. Typical kinetic traces under both limiting cases are given in Figure 3A.

The results demonstrate that the overall autoxidation of *NO is according to reaction 1, and therefore, the rate law for the autoxidation of *NO is:

$$-\frac{1}{4} \frac{d[*NO]}{dt} = -\frac{d[O_2]}{dt} = \frac{1}{4} \frac{d[NO_2^-]}{dt} = k_1[*NO]^2[O_2] \quad (2)$$

In the presence of excess of O₂ over *NO, the rate law is d[NO₂⁻]/dt = -d[*NO]/dt = k_{obs}[*NO]² and k_{obs} = 4k₁[O₂]. From Figure 1, one calculates that k₁ = k_{obs}/4 = (2.88 ± 0.02) × 10⁶ M⁻² s⁻¹. Under excess concentrations of *NO over O₂ the rate law is d[NO₂⁻]/4dt = -d[O₂]/dt = k'_{obs}[O₂] where k'_{obs} = k₁[*NO]². From Figure 2, one obtains k₁ = (2.9 ± 0.1) × 10⁶ M⁻² s⁻¹, which is in excellent agreement with the value of k₁ obtained under limiting concentrations of *NO.

The present measured rate constants are compared to the literature values in Table 2. In the presence of excess concentrations of *NO over O₂, we and others obtained a value in the range of k₁ = (2.3 ± 0.6) × 10⁶ M⁻² s⁻¹, except for the determination of Wink et al.,¹⁶ who reported a value of (4.8 ± 1.0) × 10⁶ M⁻¹ s⁻¹ (Table 2). This determination¹⁶ was carried out at 216 nm, where the light source had already about 5% or more scattered light.²⁵ Furthermore, the solutions of *NO are contaminated with nitrite, which causes through an inner filter effect an increase in the percentage of the scattered light. Therefore, the measured yield of the formation of nitrite is much lower than expected, which led Wink et al.¹⁶ to assume that Δε₂₁₆ = 1000 M⁻¹ cm⁻¹. However, *NO does not absorb at 216 nm,³⁰ and for NO₂⁻ we determined directly ε₂₁₆ = 4900 M⁻¹ cm⁻¹. The scattered light also affects the measured first-

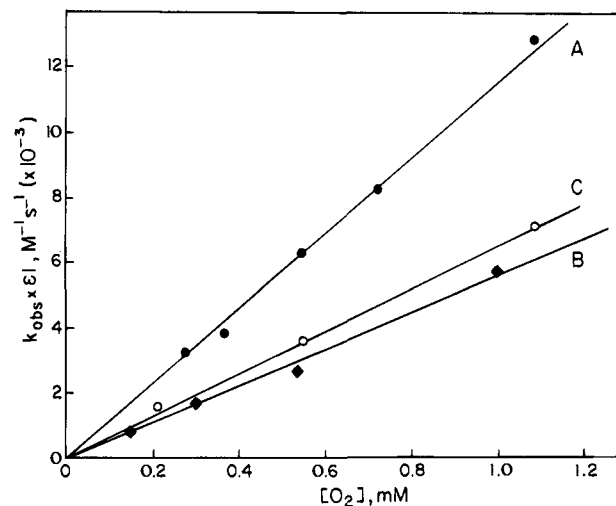
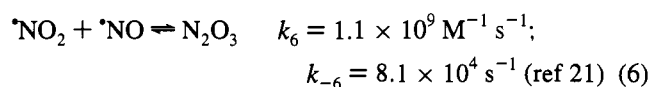
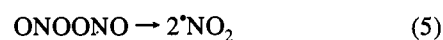
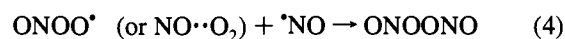
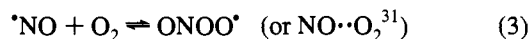


Figure 1. The observed second-order rate constant of the formation of the oxidation product in the *NO/O₂ system as a function of [O₂] at pH 7.4 (1.6 mM phosphate buffer): (A, ●) the formation of nitrite as measured at 216 nm (ε = 4900 M⁻¹ cm⁻¹) in the presence of 16.4 μM *NO; (B, ◆) the formation of ferricyanide as measured at 420 nm (ε = 1000 M⁻¹ cm⁻¹) in the presence of 65–92 μM *NO and 50 mM ferrocyanide (at initial low concentrations of O₂, [O₂]_{average} = [O₂]₀ - [*NO]); (C, ○) the formation of ABTS⁺ as measured at 660 nm (ε = 12 000 M⁻¹ cm⁻¹) in the presence of 19–39 μM *NO and 3–6 mM ABTS.

and second-order rate constants of the formation of nitrite, and the first-order rate constant is higher than expected, whereas that of the second-order rate constant is smaller than expected.²⁵

The detailed mechanism of this process can be described by reactions 3–7. In a very recent paper by McKee,³¹ it has been shown that ONOONO is formed in a concerted step from *NO and NO••O₂, a weakly bound complex of *NO and O₂, rather than from the nitrosyldioxy radical (ONO•).



We assume that *NO₂ dimerizes to O₂NNO₂ and not to ONOONO, and this process was neglected as reaction 6 followed by reaction 7 predominate under all conditions studied. Assuming that the rate-determining step is the formation of ONOONO or assuming the steady state approximation for all intermediates, rate eq 8 is obtained (see Appendix A):

$$-\frac{d[*NO]}{dt} = \frac{4k_3k_4[O_2][*NO]^2}{k_{-3} + k_4[*NO]} \quad (8)$$

According to all studies, the decay of *NO in aqueous solutions was first order in [O₂] and second order in [*NO].^{10–16} In order to get third-order kinetics from the above suggested mechanisms, one has to assume that under all experimental

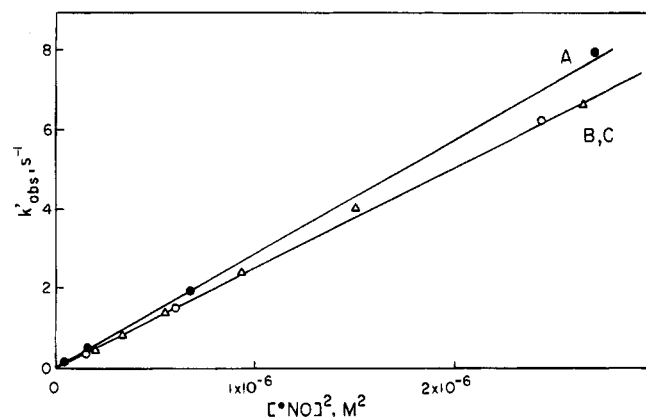


Figure 2. The observed first-order rate constant of the formation of the oxidation product in the $\cdot\text{NO}/\text{O}_2$ system as a function of $[\cdot\text{NO}]^2$ at pH 7.4 (1.6 mM phosphate buffer): (A, \bullet) the formation of nitrite in the presence of 54.5–109 μM O_2 ; (B, Δ) the formation of ferricyanide in the presence of 68.6–109 μM O_2 and 50 mM ferrocyanide; and (C, \circ) the formation of ABTS^+ in the presence of 21.8 μM O_2 and 1.1 mM ABTS .

conditions $k_{-3} > k_4[\cdot\text{NO}]$, and hence rate eq 8 reduces to rate eq 2, where $k_1 = k_3k_4/k_{-3}$. Since the concentrations of $\cdot\text{NO}$ did not exceed 1.7 mM, one calculates that $k_{-3}/k_4 > 1.7 \times 10^{-3}$ M. Furthermore, as $k_3k_4/k_{-3} = (2.9 \pm 0.1) \times 10^6 \text{ M}^{-2} \text{ s}^{-1}$, one can put lower limits for $k_3 > 5 \times 10^3 \text{ M}^{-1} \text{ s}^{-1}$. Simulation of the mechanism was carried out, and the best fit to the experimental curves given in Figure 1A is for $k_3 \geq 1 \times 10^6 \text{ M}^{-1} \text{ s}^{-1}$, $k_{-3} \geq 2 \times 10^5 \text{ s}^{-1}$ ($k_3/k_{-3} \leq 5 \text{ M}^{-1}$), $k_4 \geq 5.8 \times 10^5 \text{ M}^{-1} \text{ s}^{-1}$, and $k_5 > 5 \times 10^3 \text{ s}^{-1}$.

Effect of Ferrocyanide and ABTS on the Rate of the Autoxidation of $\cdot\text{NO}$. The reaction of $\cdot\text{NO}$ with O_2 generates an intermediate that oxidizes ferrocyanide and ABTS. These substrates also are known to react directly with $\cdot\text{NO}_2$. Using the pulse radiolysis technique, we measured the rate constants of the reaction of $\cdot\text{NO}_2$ with ferrocyanide and ABTS at pH 7.4 (5 mM phosphate buffer) to be $(2.1 \pm 0.1) \times 10^6$ and $(2.8 \pm 0.1) \times 10^7 \text{ M}^{-1} \text{ s}^{-1}$, respectively. The rate constants of the reactions of these substrates with N_2O_4 or N_2O_3 are unknown.

The $\cdot\text{NO}/\text{O}_2$ /Ferrocyanide System. The rate of formation of ferricyanide under limiting concentrations of $\cdot\text{NO}$ obeyed a second-order rate law. The yield of ferricyanide increased and the rate of its formation decreased with the increase in $[\text{Fe}(\text{CN})_6^{4-}]_0$ and with the decrease in [phosphate (Pi)] and $[\text{OH}^-]$ (Table 3). The observed second-order rate constant was linearly dependent on $[\text{O}_2]$ (Figure 1B), with a slope of $(5.5 \pm 0.3) \times 10^6 \text{ M}^{-2} \text{ s}^{-1}$. The yield of ferricyanide reached a plateau value at $[\text{Fe}(\text{CN})_6^{4-}]_0 > 50 \text{ mM}$, and $\Delta[\text{Fe}(\text{CN})_6^{3-}]/[\cdot\text{NO}]_0 = 0.84 \pm 0.03$.

In the presence of an excess of $\cdot\text{NO}$ over O_2 , the rate of formation of ferricyanide was first order. The yield of ferricyanide increased with the increase in $[\text{Fe}(\text{CN})_6^{4-}]_0$ and with the decrease in [Pi], but the rate of the reaction was unaffected by these variables (Table 3). A plateau value could not be reached. Plots of $1/[\text{Fe}(\text{CN})_6^{3-}]_{\text{final}}$ as a function of $1/[\text{Fe}(\text{CN})_6^{4-}]_0$ at two different initial concentrations of $\cdot\text{NO}$ yield straight lines (Figure 4). The reciprocal of the intercepts are the final oxidation yields, and hence $\Delta[\text{Fe}(\text{CN})_6^{3-}]/[\text{O}_2]_0 = 1.8 \pm 0.2$. The observed first-order rate constant was linearly dependent on $[\text{NO}]^2$ (Figure 2B), yielding a slope of $(2.5 \pm 0.1) \times 10^6 \text{ M}^{-2} \text{ s}^{-1}$. The results summarized in Table 3 indicate that both HPO_4^{2-} and OH^- enhance a process which competes with the oxidation of ferrocyanide. Typical kinetic traces under both limiting cases are given in Figure 3B.

The $\cdot\text{NO}/\text{O}_2$ /ABTS System. Under limiting concentrations

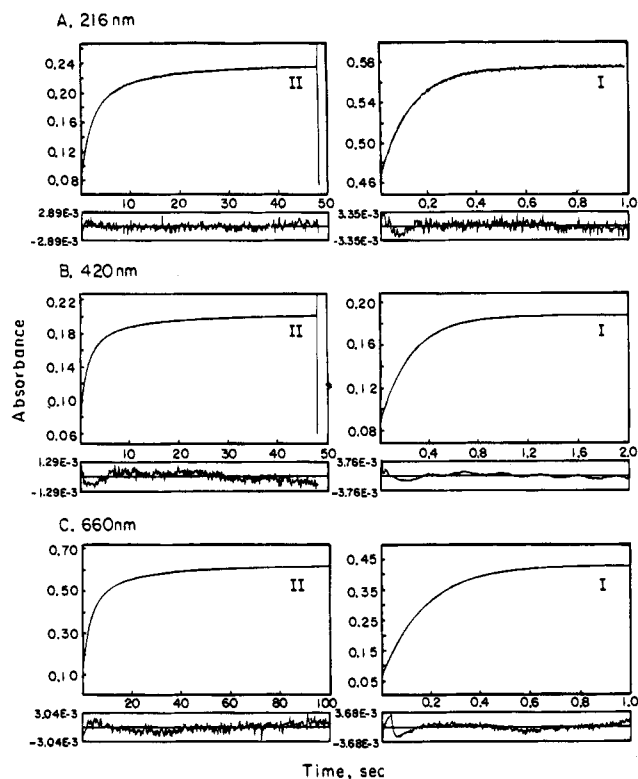


Figure 3. Typical kinetic traces of the formation of the oxidized product in the $\cdot\text{NO}/\text{O}_2$ system under limiting concentrations of $\cdot\text{NO}$ (I) and O_2 (II) at pH 7.4 (1.5–2 mM phosphate). A: (I) $[\text{O}_2]_0 = 5.45 \mu\text{M}$, $[\cdot\text{NO}]_0 = 1.64 \text{ mM}$; $\Delta\text{OD}_{216}(\text{final}) = 0.162 \pm 0.000346$; $k(2\text{nd}) = 2.62 \pm 0.0109 \text{ s}^{-1}$, normal variance 4.66×10^{-7} . (II) $[\text{O}_2]_0 = 1.09 \text{ mM}$, $[\cdot\text{NO}]_0 = 32.9 \mu\text{M}$; $\Delta\text{OD}_{216}(\text{final}) = 0.108 \pm 0.000315$; $k(1\text{st}) = 7.82 \pm 0.0392 \text{ s}^{-1}$, normal variance 1.22×10^{-6} . B: (I) $[\text{O}_2]_0 = 68.6 \mu\text{M}$, $[\cdot\text{NO}]_0 = 1.29 \text{ mM}$, $[\text{Fe}(\text{CN})_6^{4-}]_0 = 50 \text{ mM}$, $\Delta\text{OD}_{420}(\text{final}) = 0.141 \pm 0.000298$; $k(2\text{nd}) = 5.29 \pm 0.0171 \text{ s}^{-1}$, normal variance 1.82×10^{-7} . (II) $[\text{O}_2]_0 = 1.09 \text{ mM}$, $[\cdot\text{NO}]_0 = 0.164 \text{ mM}$, $[\text{Fe}(\text{CN})_6^{4-}]_0 = 50 \text{ mM}$, $\Delta\text{OD}_{420}(\text{final}) = 0.10 \pm 0.000179$; $k(1\text{st}) = 3.97 \pm 0.0121 \text{ s}^{-1}$, normal variance 3.86×10^{-7} . C: (I) $[\text{O}_2]_0 = 21.8 \mu\text{M}$, $[\cdot\text{NO}]_0 = 1.56 \text{ mM}$, $[\text{ABTS}]_0 = 0.54 \text{ mM}$, $\Delta\text{OD}_{660}(\text{final}) = 0.569 \pm 0.000584$; $k(2\text{nd}) = 0.546 \pm 0.000908 \text{ s}^{-1}$, normal variance 8.23×10^{-7} . (II) $[\text{O}_2]_0 = 1.09 \text{ mM}$, $[\cdot\text{NO}]_0 = 78 \mu\text{M}$; $[\text{ABTS}]_0 = 0.69 \text{ mM}$, $\Delta\text{OD}_{660}(\text{final}) = 0.362 \pm 0.000222$; $k(1\text{st}) = 5.79 \pm 0.00697 \text{ s}^{-1}$, normal variance 8.27×10^{-7} .

of $\cdot\text{NO}$, the rate of formation of ABTS^+ was second order, and the yield of ABTS^+ reached a plateau at $[\text{ABTS}]_0 > [\cdot\text{NO}]_0$, and decreased with the increase in [Pi] at pH 7.4. When [Pi] increased from 1.6 to 160 mM, the yield of ABTS^+ decreased by about 30%. The yield of ABTS^+ was linear with $[\cdot\text{NO}]_0$, and $\Delta[\text{ABTS}^+]/[\cdot\text{NO}]_0 = 0.60 \pm 0.02$. The observed second-order rate constant was linearly dependent on $[\text{O}_2]_0$ (Figure 1C), yielding a slope of $(6.4 \pm 0.5) \times 10^6 \text{ M}^{-2} \text{ s}^{-1}$.

In the presence of an excess of $\cdot\text{NO}$ over O_2 , the formation of ABTS^+ was first order. The yield of ABTS^+ reached a plateau at $[\text{ABTS}]_0 > 60 \mu\text{M}$, and $\Delta[\text{ABTS}^+]/[\text{O}_2]_0 = 1.32 \pm 0.05$. The observed first-order rate constant was linearly dependent on $[\text{NO}]^2$ (Figure 2C), yielding a slope of $(2.5 \pm 0.1) \times 10^6 \text{ M}^{-2} \text{ s}^{-1}$. Typical kinetic traces under both limiting cases are given in Figure 3B. In the presence of an excess of $\cdot\text{NO}$ over O_2 , the radical cation decayed very slowly via a first-order reaction. The observed first-order rate constant was linear with $[\cdot\text{NO}]_0$, yielding a second-order rate constant of $12.3 \pm 0.2 \text{ M}^{-1} \text{ s}^{-1}$. We attribute this decay to the reaction of ABTS^+ with $\cdot\text{NO}$ either to form a non-absorbing adduct or to yield back ABTS and nitrite. It should be pointed out that the rate of this process is surprisingly slow for a radical–radical reaction. However, we have no alternative explanation for this process.

Table 2. Rate Constants for Autoxidation of *NO at 22–25 °C

ref	[*NO] ₀ > [O ₂] ₀ k ₁ (10 ⁶ M ⁻² s ⁻¹)	[O ₂] ₀ > [*NO] ₀ 4k ₁ (10 ⁶ M ⁻² s ⁻¹)	kinetic method
present work	2.9 ± 0.1 (pH 7.4)	11.5 ± 0.06 (pH 1.7–11.7)	stopped-flow absorb at 216 nm
Pogrebnyaya et al. ¹⁰		8.8 ± 0.4	continuous-flow conductivity
Awad et al. ¹¹	2.1 (pH 1.22)	8.4 (pH 1.22)	stopped-flow absorb at 354 nm
	2.2	9.6 (pH 12.7)	
Lewis et al. ¹³		8.4 ± 1.6 (pH 4.9–7.4)	conductivity
Khartonov et al. ¹⁵	1.6 ± 0.1	6.3 ± 0.4	chemiluminescence stopped-flow pH indicator
Wink et al. ¹⁶	4.8 ± 1.0 (pH 7.4) ^a	6.9 4k ₁ /Δε ₂₁₆ = (6.3 ± 1.2) × 10 ³ ^a (pH 7.4) 31 ± 5.9 (Δε ₂₁₆ = 4900 M ⁻¹ cm ⁻¹) 6.3 ± 1.2 (Δε ₂₁₆ = 1000 M ⁻¹ cm ⁻¹) ^b	absorb at 354 nm stopped-flow absorb at 216 nm
Pires et al. ¹⁴		6.4 ± 0.8 (pH 1.5) 10.7 ± 1.3 (recalculated from the plot given at pH 1.5) ^c	stopped-flow absorb at 371 nm

^a Values are too high due to scattered light.²⁵ ^b The authors used Δε₂₁₆ = 1000 M⁻¹ cm⁻¹ to match with their yield, which was too low due to scattered light. A value of 4900 M⁻¹ cm⁻¹ should have been used, which also indicates that the rate constants are too high due to scattered light.²⁵ ^c The plot in Figure 2 of ref 14 was recalculated by us using the same rate equation given in ref 14. A value of (1.07 ± 0.13) × 10⁷ M⁻² s⁻¹ rather than (6.4 ± 0.8) × 10⁶ M⁻² s⁻¹ was obtained.

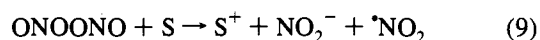
Table 3. The Effect of pH and Buffer on the Oxidation Yield and Rate of Formation of Ferricyanide in the *NO/O₂ System

buffer	[buffer], mM	pH	ΔOD ₄₂₀ ^a	k _{obs} , s ⁻¹
acetate	5	4.8	0.128	4.9
phosphate	1.5	5.9	0.121	6.0
phosphate	90	5.9	0.110	6.5
phosphate	1.5	6.9	0.131	6.3
phosphate	1.5	7.4	0.127	5.8
phosphate	16	7.4	0.109	5.5
phosphate	160	7.4	0.068	6.2
phosphate	480	7.4	0.05	7.4
HEPS	1.5	7.2	0.121	6.9
MOPS	1.5	7.4	0.135	6.0
phosphate	1.5	7.9	0.125	6.3
phosphate	90	7.9	0.055	7.6
borate	5	9.4	0.120	6.7
		10.5	0.067	9.6
		11.8	0.038	11.7
phosphate [#]	0.85	7.4	0.101	4.2
phosphate [#]	50	7.4	0.046	4.3
phosphate [#]	100	7.4	0.023	4.1

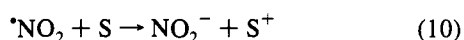
^a The change in the absorbance at the end of the reaction. All solutions contained 50 mM Fe(CN)₆⁴⁻, 0.164 mM *NO, and 1.09 mM O₂, except those marked with (#), which contained 50 mM Fe(CN)₆⁴⁻, 1.29 mM *NO, and 68.6 μM O₂.

Some support for this slow reaction is the stability of ABTS⁺ in the presence of oxygen in contrast to most organic free radicals.

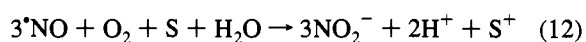
The Effect of Scavengers Reacting with Intermediates on the Rate of the Autoxidation. When a scavenger (S) reacts with ONOONO via reaction 9,



*NO₂ may either oxidize another scavenger (reaction 10) or decompose via reactions 6 and 7,



and the stoichiometry of the whole oxidation process will be given by either eqs 11 or 12, respectively.



If the rate-determining step in both cases is the formation of

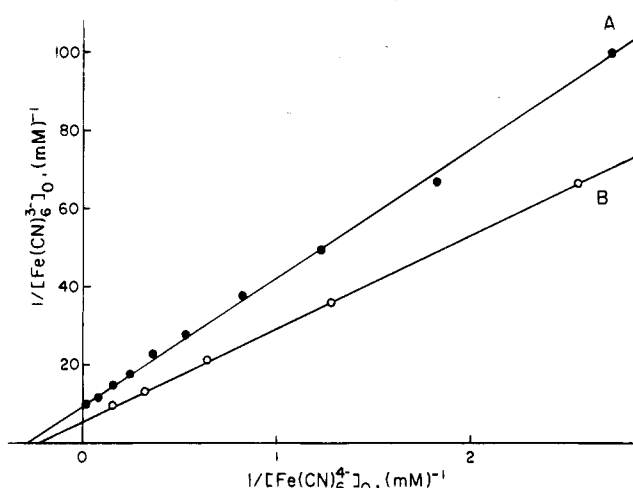


Figure 4. Double reciprocal plot of the yield of ferricyanide varying the concentration of ferrocyanide in the presence of A (○), 1.64 mM *NO and 0.109 mM O₂, and B (●), 1.29 mM *NO and 68.6 μM O₂. All solutions contained 1.6 mM phosphate buffer at pH 7.4.

ONOONO, and $k_9[\text{S}]_0 > k_5$, the third-order rate constant under limiting concentrations of *NO according to reaction 11 will be given by $2k_3k_4/k_{-3}$, and according to reaction 12 by $3k_3k_4/k_{-3}$ (see Appendix B). If S does not react with ONOONO, but with *NO₂ (reaction 10) or with N₂O₃ (reaction 13),



the stoichiometry of the whole oxidation process will be given by eq 11. When $k_{10}[\text{S}]_0 > k_6k_7[\text{NO}]_0/(k_{-6} + k_7)$ or when $k_{13}[\text{S}]_0 > k_7$, the third-order rate constant under limiting concentrations of *NO will be given by $2k_3k_4/k_{-3}$ (see Appendix B).

The third-order rate constant under limiting concentrations of O₂ will not be affected by any of the scavengers reacting with ONOONO or *NO₂ or N₂O₃, and will be given by k_3k_4/k_{-3} . In this case the rate of the reaction is determined by the rate of the disappearance of O₂, and therefore will not be affected by reactions occurring after the formation of ONOONO. The alternative oxidation pathways are summarized in Table 4.

The third-order rate constant obtained in the presence of ferrocyanide and ABTS under limiting concentrations of *NO is about half the value obtained in their absence (Figure 1), whereas under limiting concentrations of O₂, it is close to the value obtained in their absence (Figure 2). This suggests that

Table 4. Alternative Pathways for the Oxidation of a Substrate by $\cdot\text{NO}/\text{O}_2$

pathway	oxidizing intermediate	net oxidation process	conditions	rate = $k[\cdot\text{NO}]^2[\text{O}_2]$	
				$k([\text{O}_2]_0 > [\cdot\text{NO}]_0)$	$k([\cdot\text{NO}]_0 > [\text{O}_2]_0)$
I (reactions 3, 4, 9)	ONOONO	$3\cdot\text{NO} + \text{O}_2 + \text{S} + \text{H}_2\text{O} \rightarrow 3\text{NO}_2^- + \text{S}^+ + 2\text{H}^+$	$k_9[\text{S}]_0 > k_5$	$3k_3k_4/k_{-3}$	k_3k_4/k_{-3}
II (reactions 3, 4, 9, 10)	ONOONO and $\cdot\text{NO}_2$	$2\cdot\text{NO} + \text{O}_2 + 2\text{S} \rightarrow 2\text{NO}_2^- + 2\text{S}^+$	$k_9[\text{S}]_0 > k_5$ and $k_{10}[\text{S}]_0 > k_6k_7[\cdot\text{NO}]/(k_{-6} + k_7)$	$2k_3k_4/k_{-3}$	k_3k_4/k_{-3}
III (reactions 3, 4, 5, 10)	$\cdot\text{NO}_2$	$2\cdot\text{NO} + \text{O}_2 + 2\text{S} \rightarrow 2\text{NO}_2^- + 2\text{S}^+$	$k_9[\text{S}]_0 < k_5$ and $k_{10}[\text{S}]_0 > k_6k_7[\cdot\text{NO}]/(k_{-6} + k_7)$	$2k_3k_4/k_{-3}$	k_3k_4/k_{-3}
IV (reactions 3, 4, 5, 6, 13)	N_2O_3	$2\cdot\text{NO} + \text{O}_2 + 2\text{S} \rightarrow 2\text{NO}_2^- + 2\text{S}^+$	$k_9[\text{S}]_0 < k_5$ and $k_{10}[\text{S}]_0 < k_6k_7[\cdot\text{NO}]/(k_{-6} + k_7)$ and $k_{13}[\text{S}]_0 > k_7$	$2k_3k_4/k_{-3}$	k_3k_4/k_{-3}

in these cases the oxidation pathways are II or III or IV (Table 4). As $\cdot\text{NO}_2$, which is the precursor of N_2O_3 , oxidizes rapidly ferrocyanide ($k_{10} = 2.1 \times 10^6 \text{ M}^{-1} \text{ s}^{-1}$) and ABTS ($k_{10} = 2.8 \times 10^7 \text{ M}^{-1} \text{ s}^{-1}$), we can conclude that in the presence of sufficient concentrations of these substrates, N_2O_3 will not be formed, and the oxidation pathway will be described by II or III (Table 4).

The results of the competitive kinetics study in the $\cdot\text{NO}/\text{O}_2$ /ferrocyanide system suggest that the oxidizing entity in the presence of ferrocyanide is $\cdot\text{NO}_2$. If we assume that $\cdot\text{NO}$ competes with ferrocyanide for $\cdot\text{NO}_2$, the yield of ferricyanide ($[\text{Fe}^{3+}]_{\text{final}}$) under limiting concentrations of O_2 will be given by eq 14.

$$[\text{Fe}^{3+}]_{\text{final}} = 2[\text{O}_2]_0 \frac{k_{10}[\text{Fe}^{2+}]_0}{\{k_{10}[\text{Fe}^{2+}]_0 + k_6k_7[\cdot\text{NO}]_0/(k_{-6} + k_7)\}} \quad (14)$$

A plot of $1/[\text{Fe}^{3+}]_{\text{final}}$ as a function of $1/[\text{Fe}^{2+}]_0$ yields a straight line, where

$$\text{slope/intercept} = k_6k_7[\cdot\text{NO}]_0/(k_{-6} + k_7)k_{10} \quad (15)$$

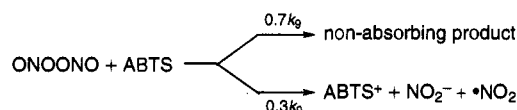
We calculated from the plots given in Figure 4 that slope/intercept = 3.7 and 4.85 mM for $[\cdot\text{NO}]_0 = 1.29$ and 1.64 mM, respectively. Thus, $k_6k_7/(k_{-6} + k_7) = (6.1 \pm 0.1) \times 10^6 \text{ M}^{-1} \text{ s}^{-1}$, which is in good agreement with $7.15 \times 10^6 \text{ M}^{-1} \text{ s}^{-1}$, which is obtained from literature values of k_6 , k_{-6} , and k_7 .²¹ Since the oxidation yields decreased with the decrease in ferrocyanide concentrations, we conclude that the hydrolysis of N_2O_3 competes efficiently with reaction 13 even in the presence of 50 mM ferrocyanide, and therefore $k_{13} < 1 \times 10^4 \text{ M}^{-1} \text{ s}^{-1}$.

Wink et al.¹⁶ assumed a competition between reaction 6 and 10 in the $\cdot\text{NO}/\text{O}_2/\text{Fe}(\text{CN})_6^{4-}$ system, ignoring reaction -6 and the hydrolysis of N_2O_3 via reaction 7. They calculated a value of " k_6 " $\sim 4 \times 10^6 \text{ M}^{-1} \text{ s}^{-1}$, which is orders of magnitude lower than $k_6 = 1.1 \times 10^9 \text{ M}^{-1} \text{ s}^{-1}$, and concluded that $\cdot\text{NO}_2$ is not the oxidizing intermediate in this system. However, as shown above, their value of " k_6 " is in good agreement with the known rate constants, if reactions -6 and 7 are taken into account. Therefore, their results indicate no need to propose any oxidizing species different from $\cdot\text{NO}_2$.

Both HPO_4^{2-} and OH^- reduce the oxidation yields of ferricyanide. Wink et al.¹⁶ have also shown that azide has an inhibitory effect in this system. It has already been demonstrated that the rate of hydrolysis of N_2O_3 is base-dependent ($k_7 = 2000 + 10^8[\text{OH}^-] \text{ s}^{-1}$),³² and most probably HPO_4^{2-} acts in a similar manner or reacts directly with N_2O_3 as azide does.³³ In the presence of X ($\text{X} = \text{OH}^-, \text{HPO}_4^{2-}, \text{N}_3^-$), $k_7 = 530 + \sum k_{13i}[\text{X}]_i$, and $k_6k_7/(k_{-6} + k_7)$ increases with the increase in $[\text{X}]$,

approaching k_6 . Thus, in the presence of X, $\cdot\text{NO}$ competes more efficiently with ferrocyanide for $\cdot\text{NO}_2$, and the oxidation yields decrease with the increase in $[\text{X}]$. The inhibitory effect of phosphate buffer has been observed by Lewis et al.¹⁷ in the presence of morpholine, but was overlooked by Wink et al.^{9,16} in the case of ferrocyanide, ABTS, and thiols. Wink et al.¹⁶ have carried most of their experiments at pH 7.4 in the presence of 0.1 M phosphate buffer. Under these conditions, phosphate should lower the oxidation yields (see Table 3). However, they reported a 1:1 ratio between S^+ (ferricyanide and ABTS^+) and $\cdot\text{NO}$.¹⁶ We have an explanation for this discrepancy in the case of ABTS where they used $\epsilon_{600}(\text{ABTS}^+) = 6600 \text{ M}^{-1} \text{ cm}^{-1}$ rather than $9600 \text{ M}^{-1} \text{ cm}^{-1}$, which is the value we determined directly using the pulse radiolysis technique.²⁶ Furthermore, from their figure (Figure 1B, ref 16), we can clearly see that the oxidation yield of ferricyanide is lower than that reported.

The results in the presence of ABTS indicate that both ONOONO and $\cdot\text{NO}_2$ are the oxidizing entities in this system (II, Table 4). The maximum oxidation yield was obtained at $[\text{ABTS}]_0 > 60 \mu\text{M}$, which is less than expected for a competition of between ABTS ($k_{10} = 2.8 \times 10^7 \text{ M}^{-1} \text{ s}^{-1}$) and $\cdot\text{NO}$ ($k = 7.15 \times 10^6 \text{ M}^{-1} \text{ s}^{-1}$)²¹ for $\cdot\text{NO}_2$. Furthermore, $\cdot\text{NO}_2$ oxidizes quantitatively ABTS to ABTS^+ , and the oxidation stoichiometries at the plateau are expected to be 1.0 and 2.0 under limiting concentrations of $\cdot\text{NO}$ and O_2 , respectively. As the observed oxidation stoichiometries are only 0.6 and 1.3, respectively, we assume that ONOONO oxidizes ABTS to ABTS^+ and in parallel to non-absorbing species as in the case of $\cdot\text{OH}$, $\text{Br}_2^-(\text{SCN})_2^-$, CCl_3O_2^- and $\text{CH}_2\text{ClO}_2^-$.³⁴



The simulation of the autoxidation of $\cdot\text{NO}$ requires that $k_5 > 5 \times 10^3 \text{ s}^{-1}$. Therefore, in order to get maximum oxidation yield at $[\text{ABTS}]_0 > 60 \mu\text{M}$, k_9 must exceed $2 \times 10^8 \text{ M}^{-1} \text{ s}^{-1}$.

Conclusions

We have demonstrated that during the autoxidation of $\cdot\text{NO}$ three potent oxidizing intermediates are formed: ONOONO, $\cdot\text{NO}_2$, and N_2O_3 . The detailed mechanism of the autoxidation of $\cdot\text{NO}$ is given by reactions 3–7.

This work demonstrates that the nature of the oxidizing intermediates formed during the autoxidation of $\cdot\text{NO}$ depends on the kind of substrate present and on its concentration. The alternative pathways for the oxidation process are summarized in Table 4 and are as follows:

(i) In the presence of an efficient scavenger of ONOONO ($k_9[\text{S}]_0 > k_5$) $\cdot\text{NO}_2$ is also formed via reaction 9. If this substrate is an efficient scavenger of $\cdot\text{NO}_2$, N_2O_3 will not be formed.

(32) Treinin, A.; Hayon, E. *J. Am. Chem. Soc.* **1970**, *92*, 5821.

(33) Williams, D. H. L. In *Nitrosation*; Williams, D. L. H., Ed.; Cambridge University Press: New York, 1988; p 5.

(34) Wolfenden, B. S.; Willson, R. L. *J. Chem. Soc., Perkin Trans. 2* **1982**, 805.

However, if $k_{10}[S]_0 < k_6k_7[*NO]_0/(k_{-6} + k_7)$, N_2O_3 will be formed and will react with S if $k_{13}[S]_0 > k_7$.

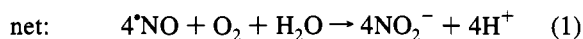
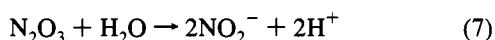
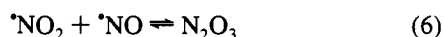
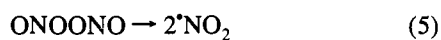
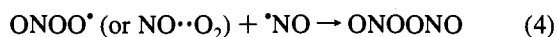
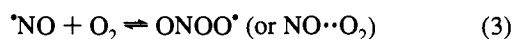
(ii) In the presence of a scavenger of $*NO_2$ ($k_9[S]_0 < k_5$), N_2O_3 will be formed only if $k_{10}[S]_0 < k_6k_7[*NO]_0/(k_{-6} + k_7)$, and will react with S provided that $k_{13}[S]_0 > k_7$.

(iii) N_2O_3 is formed and may be responsible for oxidation only in cases where $k_{10}[S]_0 < k_6k_7[*NO]_0/(k_{-6} + k_7)$ and $k_{13}[S]_0 > k_7$.

In all studies carried out so far, the rate-determining step of the oxidation and nitrosation of various substrates by $*NO/O_2$ has been shown to be the formation of ONOONO. This suggests that the first step of the autoxidation process forms a weak oxidant. Though ONOO* is a mild oxidant with a reduction potential of 0.44 V,³⁵ one expects that as a free radical it will be able to participate in some of the processes. As this is not the case, one has to conclude that the reaction of $*NO$ with O_2 (reaction 3) forms a weakly bound complex $NO\cdots O_2$ rather than ONOO*, as has been suggested by McKee.³¹

Acknowledgment. This research was supported by The Council for Tobacco Research, Grant No. 4129, and by The Israel Science Foundation.

Appendix A: Rate Equation Obtained for the Autoxidation of $*NO$



$$R_1 = -d[O_2]/dt = k_3[*NO][O_2] - k_{-3}[ONOONO^*]$$

A steady state approximation is assumed for ONOO*. Thus,

$$R_2 = d[ONOONO^*]/dt = k_3[*NO][O_2] - k_{-3}[ONOONO^*] + k_4[ONOONO^*][*NO] = 0$$

$$\Rightarrow [ONOONO^*]_{s,s} = k_3[*NO][O_2]/(k_{-3} + k_4[*NO])$$

Substituting $[ONOONO^*]_{s,s}$ into R_1 yields

(35) Beckman, J. S.; Koppenol, W. In *Biology of Nitric Oxide*; Moncada, S., Marletta, M. A., Hibbs, J. B., Jr., Higgs, E. A., Eds.; Portland Press: London, 1992; Vol 2, p 131.

$$R_1 = -d[O_2] = k_3k_4[*NO]^2[O_2]/(k_{-3} + k_4[*NO])$$

Due to the stoichiometry of the whole oxidation process (reaction 1)

$$-\frac{1}{4} \frac{d[*NO]}{dt} = -\frac{d[O_2]}{dt} = \frac{1}{4} \frac{d[NO_2^-]}{dt} \quad (2)$$

and therefore

$$-d[*NO]/dt = 4k_3k_4[*NO]^2[O_2]/(k_{-3} + k_4[*NO])$$

Appendix B: Rate Equation Obtained for Oxidation Pathways I, II, III, and IV

(i) Oxidation pathways II, III and IV yield the same net reaction 11.



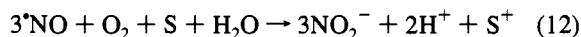
Therefore,

$$-\frac{1}{2} \frac{d[*NO]}{dt} = -\frac{d[O_2]}{dt} = \frac{1}{2} \frac{d[NO_2^-]}{dt} = \frac{1}{2} \frac{d[S^+]}{dt}$$

The rate of the decay of O_2 is unaffected by the presence of S (R_1 as obtained in Appendix A), and therefore

$$-d[*NO]/dt = d[S^+]/dt = 2k_3k_4[*NO]^2[O_2]/(k_{-3} + k_4[*NO])$$

(ii) Oxidation pathway I yields the net reaction 12.



Therefore,

$$-\frac{1}{3} \frac{d[*NO]}{dt} = -\frac{d[O_2]}{dt} = \frac{1}{3} \frac{d[NO_2^-]}{dt} = \frac{d[S^+]}{dt}$$

The rate of the decay of O_2 is unaffected by the presence of S (R_1 as obtained in Appendix A), and therefore

$$-d[S^+]/dt = k_3k_4[*NO]^2[O_2]/(k_{-3} + k_4[*NO])$$

and

$$-d[*NO]/dt = 3k_3k_4[*NO]^2[O_2]/(k_{-3} + k_4[*NO])$$

JA952045J